DALTON
FULL PAPER

Structure, optical and magnetic behaviour of *meso*-tetraphenylporphyrinatoiron(III) tetracyanoethenide, $[Fe^{III}(TPP)]^{+}[TCNE]^{\cdot -}$ †

Shinji Mikami,[a] Ken-ichi Sugiura,*[a] Tatsuo Maruta,[b] Yonezo Maeda,[b] Masaaki Ohba,[bc] Naoki Usuki,[b] Hisashi Ōkawa,[b] Tomoyuki Akutagawa,[cd] Sadafumi Nisihara,[d] Takayoshi Nakamura,[d] Kentaro Iwasaki,[e] Nobuyuki Miyazaki,[e] Shojun Hino,[e] Eiji Asato,[f] Joel S. Miller *[g] and Yoshiteru Sakata *[a]

[a] *The Institute of Scientific and Industrial Research (ISIR), Osaka University, 8-1 Mihogaoka, Ibaraki, Osaka 567-0047, Japan. E-mail: sugiura@sanken.osaka-u.ac.jp;sakata@sanken.osaka-u.ac.jp*
[b] *Department of Chemistry, Faculty of Sciences, Kyushu University, Hakozaki-ku 6-10-1, Fukuoka 812-8581, Japan*
[c] *PREST, Japan Science and Technology Corporation (JST), Kawaguchi Center Building 1–8, Honcho 4-chome, Kawaguchi City, Saitama 332-0012, Japan*
[d] *Research Institute for Electronic Science, Hokkaido University, Sapporo 060-0812, Japan*
[e] *Faculty of Engineering, Chiba University, Inageku, Chiba 263-8522, Japan*
[f] *Department of Chemistry, Biology, and Marine Science, University of the Ryukyus, Nishihara-cho, Okinawa 903-0213, Japan*
[g] *Department of Chemistry, University of Utah, Salt Lake City, UT 84112-0850, USA. E-mail: jsmiller@chemistry.chem.utah.edu*

Received 2nd October 2000, Accepted 4th December 2000
First published as an Advance Article on the web 18th January 2001

The direct redox reaction between tetracyanoethylene (TCNE) and *meso*-tetraphenylporphyrinatoiron(II), $[Fe^{II}(TPP)]$, formed the electron transfer salt (ETS) $[Fe^{III}(TPP)][TCNE]$, which has been structurally, spectroscopically, and magnetically characterized. It has an extended one-dimensional linear chain with coordination polymer motif comprised of $[Fe^{III}(TPP)]^{+}$ and bridging μ-$[TCNE]^{\cdot -}$ with Fe–N^{TCNE} distance 1.889(2) Å. This coordination geometry is consistent with a low-spin iron(III) ion, *i.e.*, one electron transfer from Fe^{II} to TCNE produces $S = 1/2$ $[Fe^{III}(TPP)]^{+}$ having a $(d_{xy})^2(d_{yz},d_{zx})^3$ configuration and $S = 1/2$ $[TCNE]^{\cdot -}$. ^{57}Fe Mössbauer data, $\delta = 0.28$ mm s^{-1} and $\Delta E = 2.19$ mm s^{-1} at 77 K, also support the low-spin state. The room temperature magnetic moment of the ETS, 1.20 μ_B, arises from two $S = 1/2$ systems having antiferromagnetic coupling, -190 cm^{-1} ($H = -2\Sigma J_{ij}\boldsymbol{S}_i\boldsymbol{S}_j$).

Introduction

Molecule-based magnetic materials have been attracting much attention as a contemporary interdisciplinary research area for over the past three decades, since the first theoretical proposal by McConnell in 1967[1] and its experimental realization.[2] A variety of magnetically coupled materials such as neutral radicals, poly-carbenes, and nitrenes, as well as ordered electron transfer salts (ETSs), have been reported.[1] ETSs constructed from porphyrinatomanganese(II) and acceptor molecules such as tetracyanoethylene (TCNE), *e.g.*, *meso*-tetraphenylporphyrinatomanganese(III) tetracyanoethenide $[Mn^{III}(TPP)]^{+}$-$[TCNE]^{\cdot -}\cdot 2C_6H_5Me$,[1a,3,4] hold a unique position in this research field, because (i) their structures are well controlled by the Mn–N^{TCNE} coordination bond to produce extended one-dimensional (1-D) chain supramolecular architectures,[1a] (ii) they display strong exchange interactions and have magnetic ordering temperatures, T_c, as high as 28 K,[5] and (iii) some have an extremely large coercive field, H_{cr}, at 2 K comparable to those of commercially used rare earth metal magnets.[6] To get further information on these ETSs as well as to obtain new magnets with enhanced physical properties, such as higher T_c and larger H_{cr}, we have varied (1) the porphyrin ligand,[5–16] (2) solvent,[13,14,17–20] (3) acceptor molecule,[8,17,21–30] and (4) metal ion.[31] In the course of these systematic studies of (1)–(3) we have developed some important guidelines for the magnets: (a) importance of uniform chain structure,[7,8,15,27,28] (b) metal bonding at a site having large spin density,[21] and (c) small Mn–NC^{TCNE} coordination bond angle for strong exchange interactions.[9,11,17,20]

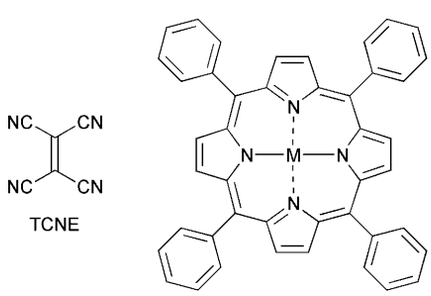

Replacing the metal ion of manganese porphyrins with other transition metals is the remaining strategy, (4),[31] as the spin multiplicity, S, correlates with T_c according to the simplest

† Electronic supplementary information (ESI) available: least-squares deviations from the porphyrin plane; plot of d(Fe–$N^{porphyrin}$) *vs.* d(Fe–N^{TCNE}). See http://www.rsc.org/suppdata/dt/b0/b007931f/

 DOI: 10.1039/b007931f

mean-field model, *i.e.*, $T_c \sim S(S + 1)$.[1d] This equation is only an approximation but is nevertheless a useful approach to obtain a molecule-based magnet with a high T_c. The most successful results were reported for $[M(C_5Me_5)_2]^+[acceptor]^{\cdot -}$ where, the $S = 1/2$ system ($M = Fe^{III}$) displays T_c 4.8 K (acceptor = TCNE)[32] and 2.55 K (acceptor = TCNQ, 7,7,8,8-tetracyano-*p*-quinodimethane),[33] respectively, whereas the $S = 1$ system ($M = Mn^{III}$) shows T_c 8.8 K (acceptor = TCNE)[34] and 6.3 K (acceptor = TCNQ).[35] Since porphyrins can incorporate many kinds of metals (M), the systematic replacement of Mn^{III} with M with differing *S* values results in higher T_c.

We selected Fe as the incorporated metal ion because Fe^{III} can have three different spin states depending on the coordination geometry: high ($S = 5/2$), intermediate ($S = 3/2$), and low ($S = 1/2$). Additionally, porphyrinatoiron(II) is sufficiently reducing to reduce TCNE.[36,37] Herein we report the result of replacing the donor molecule of the ETS, $[Mn^{II}(TPP)]$, by *meso*-tetraphenylporphyrinatoiron(II), the synthesis and structural, electronic, and spectroscopic properties of *meso*-tetraphenylporphyrinatoiron(III) tetracyanoethenide, $[Fe^{III}\text{-}TPP]^+[TCNE]^{\cdot -}\cdot 2PhCl$.

Results and discussion

Synthesis

In accord with $[Mn^{III}(por)]^+[acceptor]^{\cdot -}$ syntheses,[3,4] the direct redox reaction between $[Fe^{II}(TPP)]$[38] and TCNE was carried out in chlorobenzene to form $[Fe^{III}(TPP)]^+[TCNE]^{\cdot -}\cdot 2PhCl$.[39] This ETS behaves as another example of a *porphyrin sponge*,[40] since it incorporates two solvent molecules, PhCl in this case. Thermogravimetric analysis (TGA) showed a weight loss attributable to all of the solvent at <180 °C, after which decomposition was observed up to 400 °C with a steady weight loss.

Structure

The X-ray analysis of $[Fe^{III}(TPP)]^+[TCNE]^{\cdot -}\cdot 2PhCl$ revealed 1-D chains comprised of alternating $[Fe^{III}(TPP)]^+$ and $[TCNE]^{\cdot -}$ with each iron being six-coordinate *trans*-μ-*N*-bound to two $[TCNE]^{\cdot -}$ (Fig. 1). Although this 1-D coordination polymeric motif is similar to those observed for magnetically ordered $[Mn^{III}(por)]^+[TCNE]^{\cdot -}$ complexes,[4] several unique characteristics attributable to iron were found. The key parameters best describing the structure of the ETS are summarized in Table 1 along with those for $[Mn^{III}(TPP)]^+\text{-}[TCNE]^{\cdot -}\cdot 2C_6H_5Me$.[4]

It is well known that the oxidation and spin states of porphyrinatoiron can be classified by its coordination geometry.[41] The Fe atom of [Fe(TPP)][TCNE]·2PhCl was assigned to have a $S = 1/2$ low-spin state, where one-electron transfer has occurred from Fe^{II}(TPP) to TCNE and to form Fe^{III} having $(d_{xy},d_{yz},d_{zx})^5$ and $[TCNE]^{\cdot -}$. Thus, the average $Fe\text{–}N^{porphyrin}$ bond distance (1.999 Å) is similar to those of other low-spin iron(III) complexes (*e.g.* 1.970–1.998 Å),[41] but shorter than those for high-spin complexes having expanded porphyrin cores (*e.g.* 2.038–2.049 Å).[41] Generally, the bond distance between Fe^{III} and the nitrogen of an axial ligand is more sensitive for determining the spin state of Fe^{III}. The observed $Fe\text{–}N^{TCNE}$ distance, 1.889(2) Å, is to the best of our knowledge, the shortest ever reported for iron(III) complexes, which range from 1.928 to 2.089 Å for low spin, 2.126 to 2.314 Å for intermediate spin, and 2.068 to 2.442 Å for high spin.[41] This is 0.416 Å shorter than the corresponding value of $[Mn^{III}(TPP)]^+\text{-}[TCNE]^{\cdot -}\cdot 2C_6H_5Me$,[4] again characteristic of low-spin Fe^{III}, and the lack of an electron in the d_{z^2} orbital. Furthermore, these results are consistent with other spectroscopic studies including Mössbauer (see below). The porphyrin core is flat within ±0.09 Å from the least squares plane, suggesting a $(d_{xy})^2(d_{yz},d_{zx})^3$ electronic configuration (see ESI Fig. S-1).[42] Recently, Silver

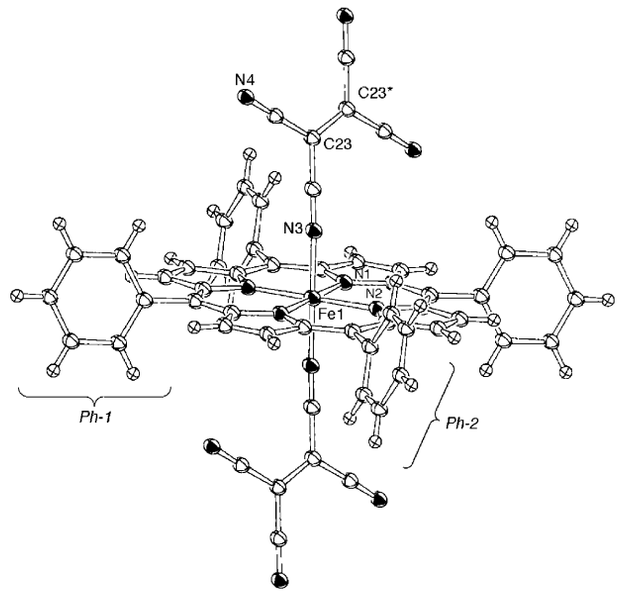

(a)

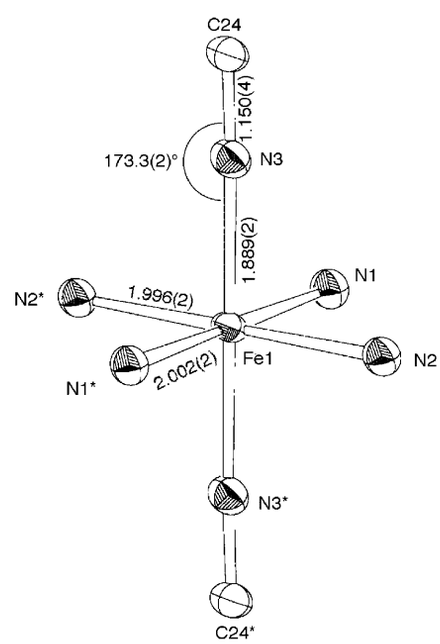

(b)

Fig. 1 ORTEP (50%) views of a segment of the 1-D chain: (a) $[TCNE]^{\cdot -}\cdots[Fe^{III}(TPP)]^+\cdots[TCNE]^{\cdot -}$, (b) the iron and six bonded nitrogen atoms. Dihedral angles between the phenyl group and the porphyrin plane: 73.78(16)° for *Ph-1* and 77.38(11)° for *Ph-2*.

et al. pointed out that the electronic configuration of low-spin Fe^{III} is easily classified by a plot of $d(Fe\text{–}N^{porphyrin})$ against $d(Fe\text{–}N^{ligand})$.[43] The value of $[Fe^{III}(TPP)]^+[TCNE]^{\cdot -}\cdot 2PhCl$ is located well within the $(d_{xy})^2(d_{yz},d_{zx})^3$ region (see ESI Fig. S-2), again supporting the low-spin description. Although the deviation of the iron atom from the porphyrin plane does not always reflect the oxidation and spin states of the complex, Fe^{III} is situated at a center of symmetry in the plane of the four porphyrin nitrogen atoms. The coordination bond angles around Fe^{III} are nearly 90° (Fig. 1(b)).

Comparing these coordination parameters with those of $[Mn^{III}(por)]^+[TCNE]^{\cdot -}$, some interesting features are revealed. The dihedral angle between the $[TCNE]^{\cdot -}$ and porphyrin mean plane, ∠P-TCNE, is nearly perpendicular, 80.39(6)°, and larger by 25.1° than that of $[Mn^{III}(TPP)]^+[TCNE]^{\cdot -}\cdot 2C_6H_5Me$ (55.3°)[4] and similar to those of $[Mn^{III}(TPP)]^+\text{-}$

Table 1 Comparison of the important structural parameters of $[Fe^{III}(TPP)]^+[TCNE]^{\bullet-}\cdot 2PhCl$ with those of $[Mn^{III}(TPP)]^+[TCNE]^{\bullet-}\cdot 2C_6H_5Me$ [a]

	$[Fe^{III}(TPP)]^+[TCNE]^{\bullet-}\cdot 2PhCl$	$[Mn^{III}(TPP)]^+[TCNE]^{\bullet-}\cdot 2C_6H_5Me$ [b]	Δ [c]
$d(M–N^{TCNE})$/Å	1.889	2.305	−0.416
$d(M–N^{porphyrin})$/Å	1.999	1.998	+0.001
d(M–M)/Å	9.628	10.116	−0.488
∠M–NC^{TCNE}/°	173.3	148.1	+25.2
∠P–TCNE/°	80.4	55.3	+25.1
d(P–P)/Å	9.45	9.28	+0.17
$d(C{=}C^{TCNE})$/Å	1.398	1.369	+0.029

[a] $d(M–N^{TCNE})$ ≡ M–N^{TCNE} coordination bond distance, $d(M–N^{porphyrin})$ ≡ average Fe–N^{porphyrin} bond distance, d(M–M) ≡ intrachain metal–metal distance, ∠M–NC^{TCNE} ≡ M–NC^{TCNE} coordination bond angle, ∠P–TCNE ≡ dihedral angle between porphyrin ligand and $[TCNE]^{\bullet-}$, d(P–P) ≡ intrachain interplanar porphyrin–porphyrin distance, and $d(C{=}C^{TCNE})$ ≡ bond distance of the central C=C of TCNE. [b] From reference 3. [c] Δ = (value of $[Mn^{III}(TPP)]^+[TCNE]^{\bullet-}\cdot 2C_6H_5Me$) −(value of $[Fe^{III}(TPP)]^+[TCNE]^{\bullet-}\cdot 2PhCl$).

Table 2 Bond distances (Å) of $[TCNE]^{\bullet-}$ for $[Fe^{III}(TPP)]^+[TCNE]^{\bullet-}\cdot 2PhCl$

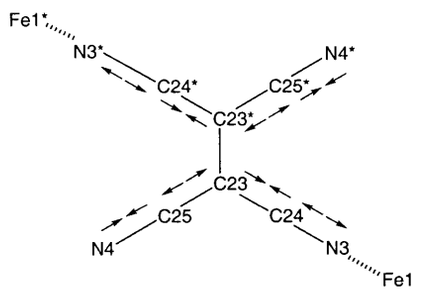

Fe–N3	1.889(2)			
N3–C24	1.150(4)	N4–C25	1.138(4)	+0.012
C23–C24	1.409(4)	C23–C25	1.426(4)	−0.017
C23–C23*	1.398(5)			

$[TCNE]^{\bullet-}\cdot 2(C_6H_4Me_2\text{-}o)$ (81.9°)[14] and $[Mn^{III}(TMeOPP)]^+$-$[TCNE]^{\bullet-}\cdot 2C_6H_5Me$ (78.1°, TMeOPP ≡ *meso*-tetrakis(4-methoxyphenyl)porphyrinate).[12] Low-spin iron(III) complexes tend to have a perpendicular coordination motif, *e.g.* 77.5 to 88.3° for $[Fe^{III}(TMesP)(5\text{-}MeHIm)_2]^+ClO_4^-$ (TMesP ≡ *meso*-tetrakis(2,4,6-trimethylphenyl)porphyrinate, 5-MeHIm ≡ 5-methylimidazole).[44] Although Scheidt and co-workers proposed steric factors for perpendicular bonding based on molecular mechanics calculations,[45] *i.e.* the repulsion between the axial ligands and the four aryl groups on the porphyrin, the system constructed from $[TCNE]^{\bullet-}$ and *meso*-tetraphenylporphyrinate has less steric repulsion. In contrast, the dihedral angle ∠P-TCNE of the $[Mn^{III}(por)]^+[TCNE]^{\bullet-}$ system freely changes from 22.3 to 88.4° depending on the crystal packing requirements and the solvents.[14] In this case, we attribute the strong π overlap to the π-d_{yz} (or π-d_{zx}) and the pπ* orbitals producing the perpendicular coordination to maximize the interaction. This is consistent with the extremely short $d(Fe–N^{TCNE})$ distance (1.889(2) Å) and the nearly linear angle ∠Fe–NC^{TCNE} (173.3(2)°). This bonding is in marked contrast to the σ overlap noted for $[Mn^{III}(por)]^+[TCNE]^{\bullet-}$ ETSs.[1k]

The intramolecular bond distances are characteristic of $[TCNE]^{\bullet-}$ (Table 2). The central C–C bond distance of the $[TCNE]^{\bullet-}$ (C23–C23*: 1.398(5) Å) also supports an ionic ground state for the complex. This distance is as expected for its 1.5 bond order, *e.g.* 1.392(9) Å for $[Fe(C_5Me_5)_2]^+[TCNE]^{\bullet-}$.[46,47] Comparing bond distances for chemically equivalent bonds, a remarkable bond alternation was found for the dicyanomethylene unit of $[TCNE]^{\bullet-}$. For example, the C≡N bond distance N3–C24 (1.150(4) Å) is 0.012 Å longer than that of N4–C25 (1.138(4) Å). In contrast, C24–C23 (1.409(4) Å) is 0.017 Å shorter than C23–C25 (1.426(4) Å). This alternation is explained by the *bond-length variation rule* proposed by Gutmann.[48] Thus, when nitrogen atom N3 coordinates to Fe^{III} the adjacent covalent bonds, N3–C24 and C23–C25, become longer and the adjacent bonds, C23–C24 and N4–C25, become shorter (see diagram in Table 2).

The uniform 1-D chain (chain *I*; Figs. 2 and 3) is surrounded by two nearest neighbouring chains (*II*) in the [100] direction, by two next neighbouring chains (*III*) in the [010] direction, and four more detached chains in the [110] and [$\bar{1}\bar{1}$1] directions (*IV* and *IV′*) (Fig. 2). Chains *I* and *II* produce a quasi 2-D sheet structure in an out-of-register manner (Fig. 3(a)).[49] The driving force for this sheet structure may be attributable to the weak π–π interaction between the phenyl groups of $[Fe^{III}(TPP)]^+$ and $[TCNE]^{\bullet-}$ which is observed for $[Mn^{III}(TPP)]^+[TCNE]^{\bullet-}$.[24] These 2-D sheets interact in the [010] direction in an in-register manner.[49] The solvent molecules, PhCl, are incorporated between the sheets. Interchain interactions such as Fe···Fe (10.937 to 17.383 Å) and Fe···$[TCNE]^{\bullet-}$ (9.940–14.724 Å) are in the range observed for $[Mn^{III}(por)]^+[TCNE]^{\bullet-}$ systems, 11.006 to 14.932 Å (Fig. 3).[4,14]

Spectroscopic studies

The ν_{CN} vibration modes of $TCNE^{n-}$ (n = 0, 1 or 2) are well known and reflect the ionicity of the molecule.[46,47] A large frequency shift to lower energy for the ν_{CN} absorptions (2206s and 2145w cm^{-1}) of $[Fe^{III}(TPP)]^+[TCNE]^{\bullet-}\cdot 2PhCl$ with respect to those for TCNE (2259 s and 2221 m cm^{-1}) supports an electron-transfer complex (Fig. 4).[46,47] Interestingly, the shifts to higher energy with respect to the values observed for non-bonded $[TCNE]^{\bullet-}$ (Fig. 4(d): 2183m and 2144s cm^{-1}) are larger than those for $[Mn^{III}(TPP)]^+[TCNE]^{\bullet-}\cdot 2C_6H_5Me$ (Fig. 4(c): 2192m and 2147s cm^{-1}).[4] Although π-d_{yz} (or π-d_{zx}) and pπ* interactions of the ETS and the resultant strong π back donation of the complex induce a low-frequency shift for the ν_{CN} vibration,[48,50] π donation from the basic $[TCNE]^{\bullet-}$ to the vacant dπ orbital of low-spin Fe^{III} is also expected for this ETS, *i.e.* a back charge transfer from $[TCNE]^{\bullet-}$ to Fe^{III} (see below).[37,51,52] The latter interaction strengthens the C≡N bond, hence a higher-frequency shift is induced. For ν_{CN} of $[Fe^{III}$-$(TPP)]^+[TCNE]^{\bullet-}2PhCl$ the latter interaction may be predominant.

In marked contrast to $[Mn^{III}(por)]^+[TCNE]^{\bullet-}$[1a] the frequencies of the ν_{CN} band for $[Fe^{III}(TPP)]^+[TCNE]^{\bullet-}\cdot 2PhCl$ showed a remarkable dependence on the temperature (Fig. 5). The absorption at 2206 cm^{-1} splits into two bands at 2220 and 2208 cm^{-1} with decrease in temperature. At the same time the intensities of the weak band at 2145 cm^{-1} and the shoulder at around 2225 cm^{-1} at room temperature increase to give distinct bands at 2155 and 2232 cm^{-1}, respectively. These changes are reversible. Although the details of this behaviour are unclear, it is attributable to the onset of a non-uniform 1-D chain and/or a phase transition,[15] and might be attributable to the short Fe–N^{TCNE} coordination bonding.

The solid state electronic absorption spectrum of $[Fe^{III}$-$(TPP)]^+[TCNE]^{\bullet-}\cdot 2PhCl$ has a Soret band at 24 000 cm^{-1} and

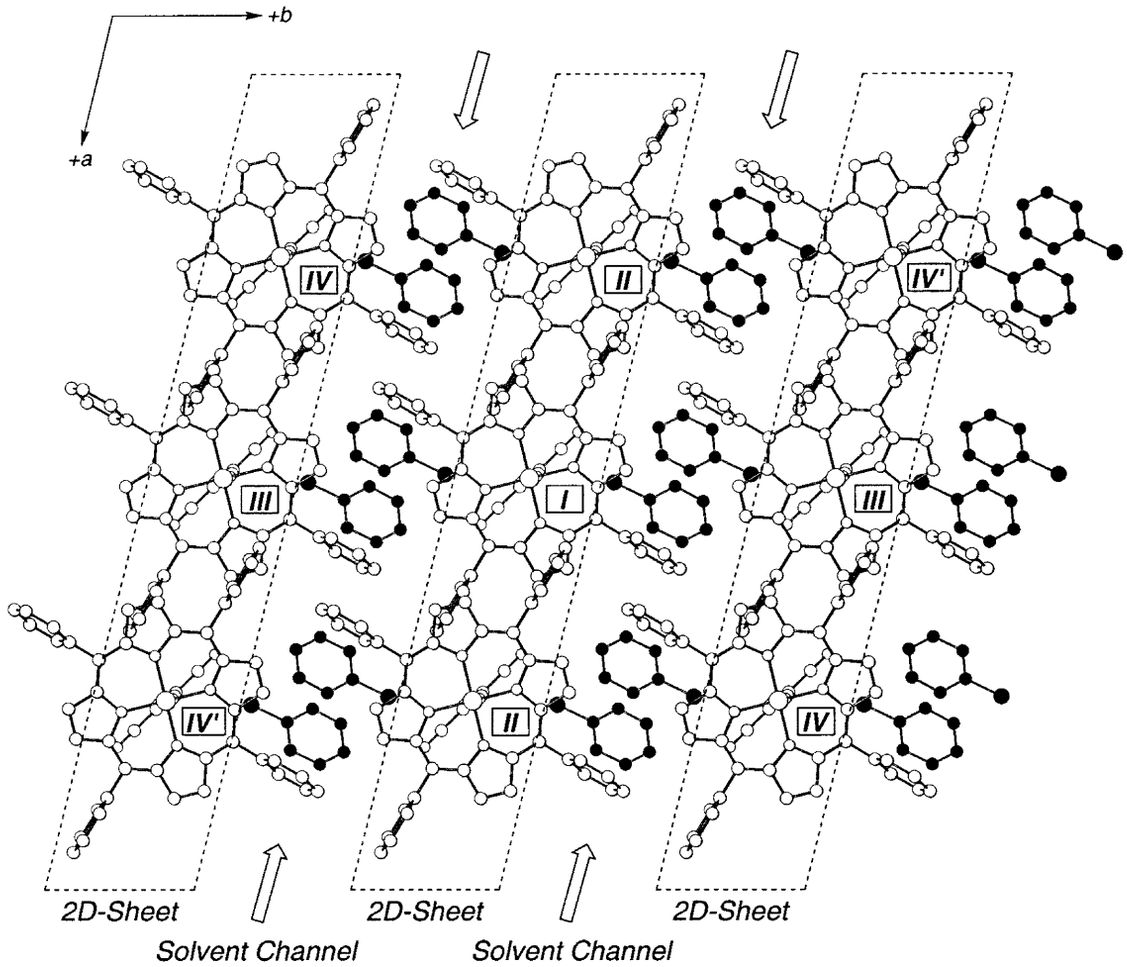

Fig. 2 Top view of the crystal packing. The 2-D sheet structure is highlighted with dashed lines and the solvent channel is shown with arrows. Solvent molecules, PhCl, are represented as black circles.

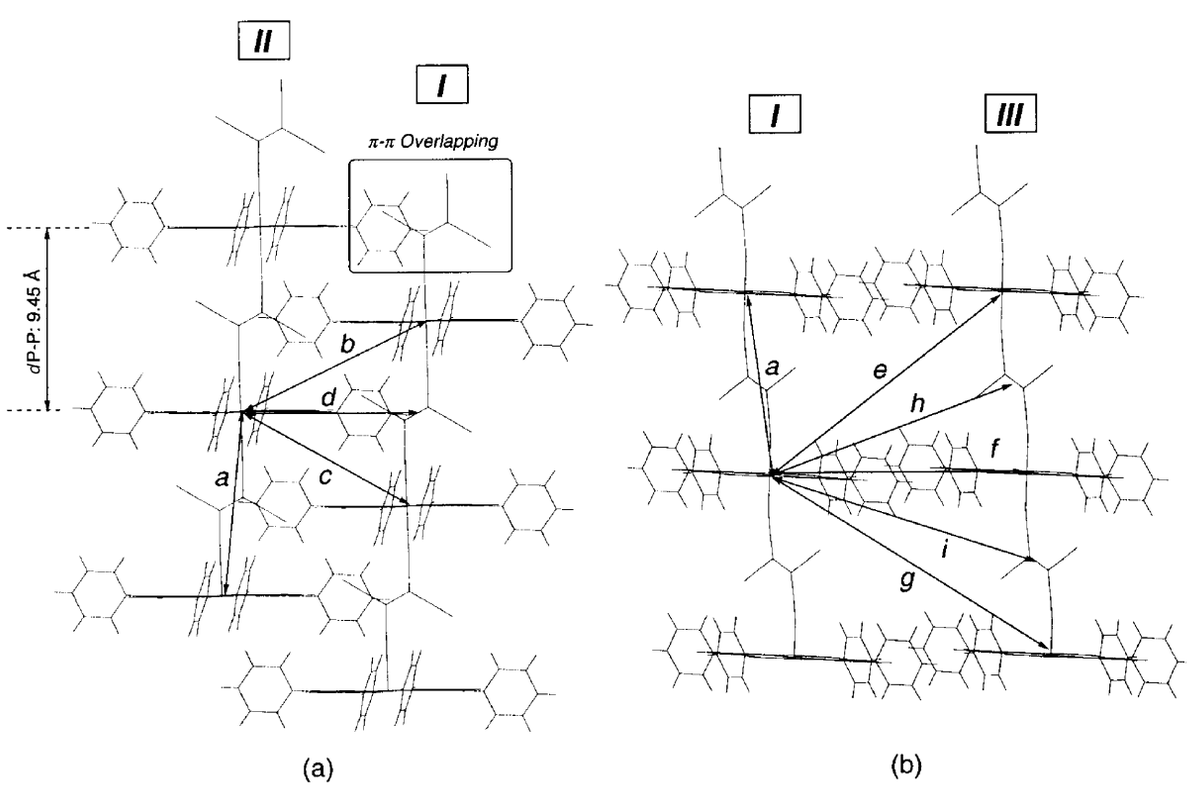

Fig. 3 Views of interchain interactions among the unique chains: (a) out-of-register interacting chains *I* and *II*, (b) in-register interacting chains *I* and *III*. The interchain π–π overlap between $[TCNE]^{\bullet -}$ and the phenyl group of $[Fe^{III}(TPP)]^{+}$ is highlighted with the square in (a). Important interactions, interchain Fe···Fe and Fe···TCNE distances: $a = 9.628$ (≡ c unit cell axis), $b = 11.124$, $c = 10.937$ (≡ a unit cell axis), $d = 9.940$, $e = 15.430$, $f = 13.320$ (≡ b unit cell axis), $g = 17.383$, $h = 13.601$, and $i = 14.724$ Å.

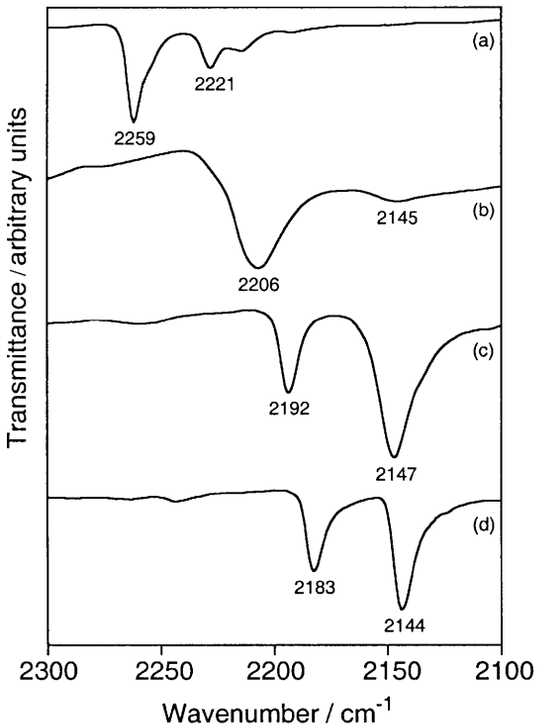

Fig. 4 IR spectra of (a) neutral TCNE, (b) $[Fe^{III}(TPP)]^{+}[TCNE]^{\bullet -}\cdot 2PhCl$, (c) $[Mn^{III}(TPP)]^{+}[TCNE]^{\bullet -}\cdot 2C_6H_5Me$, and (d) $[Fe^{III}(C_5Me_5)_2]^{+}[TCNE]^{\bullet -}$.

two bands at 19 500 and 17 900 cm^{-1} attributable to the Q band of the porphyrin ligand.[53] The band at 6500 cm^{-1} was characterized as a back charge transfer transition, *i.e.* $[TCNE]^{\bullet -} \rightarrow [Fe^{III}(TPP)]^{+}$ (see above).

Mössbauer spectra. The oxidation state and the spin multiplicity of the iron have also been determined from the ^{57}Fe Mössbauer spectrum in zero applied magnetic field with isomer shifts normalized to iron foil at room temperature. The spectrum showed a quadrupole doublet that was magnetically broadened even at room temperature, and the left absorption is broader than the right one (Fig. 6). The quadrupole splitting increased slightly with increasing temperature, with isomer shifts of $\delta = 0.21$ mm s^{-1} and quadrupole splitting of $\Delta E = 2.26$ mm s^{-1} at 290 K, $\delta = 0.28$ mm s^{-1} and $\Delta E = 2.19$ mm s^{-1} at 77 K (Fig. 6). These values are typical for low-spin iron(III) ions.[54] The values are plotted *vs.* isomer shift and quadrupole splitting, the Maeda map,[55] together with the reported values in Fig. 7. The values of $[Fe^{III}(TPP)]^{+}[TCNE]^{\bullet -}\cdot 2PhCl$ are located within a circle specified by low-spin iron(III) complexes. The charge and spin states of the ETS were also confirmed from X-ray photoelectron spectroscopy[56] and electron paramagnetic resonance.[57]

Magnetic behaviour

The susceptibility (χ) of $[Fe^{III}(TPP)]^{+}[TCNE]^{\bullet -}\cdot 2PhCl$ was measured from 2 to 300 K. The observed effective moment, μ_{eff}, is 1.20 μ_B at 300 K, which is less than that expected for independent isotropic $g = 2$, $S = 1/2$ low-spin Fe^{III} and $S = 1/2$ $[TCNE]^{\bullet -}$, 2.45 μ_B. This is attributable to significant antiferromagnetic coupling interaction through the Fe–N^{TCNE} coordination bond. The μ_{eff} decreases with decreasing temperature and is 0.43 μ_B at 2 K (Fig. 8). χT can be fitted by the 1-D Ising equation, (1), where N = Avogadro number, β = Bohr

$$\chi = \frac{Ng^2\beta^2}{12k_B(T-\theta)} \times \frac{e^{4K} + (2 + K^{-1})e^{2K} - K^{-1}e^{-2K} + 5}{e^{2K} + e^{-2K} + 2} \times (1-\rho) + \frac{Ng^2\beta}{6k_BT} \times \rho + Na \quad (1)$$

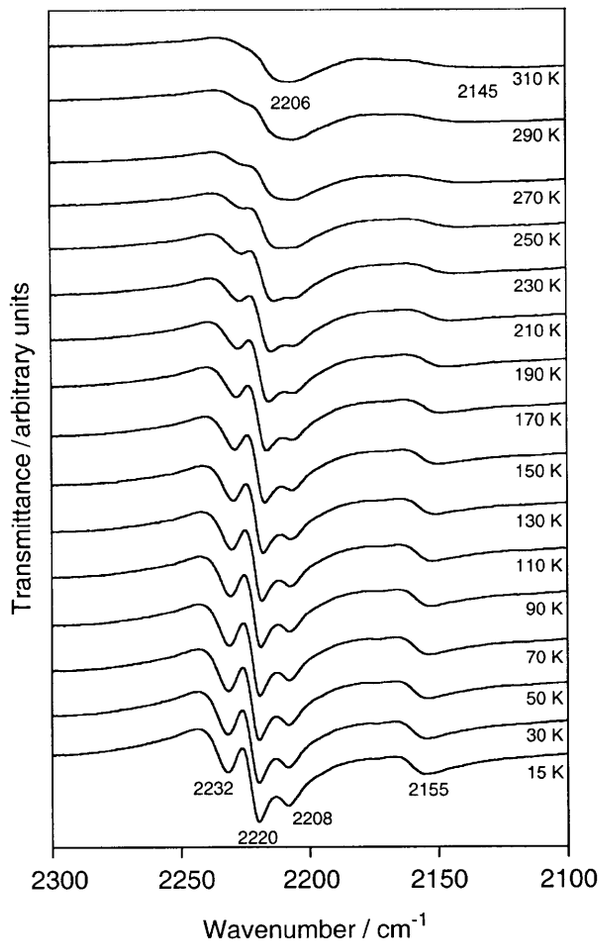

Fig. 5 Temperature dependent IR spectra of $[Fe^{III}(TPP)]^{+}[TCNE]^{\bullet -}\cdot 2PhCl$ measured from 15 to 310 K.

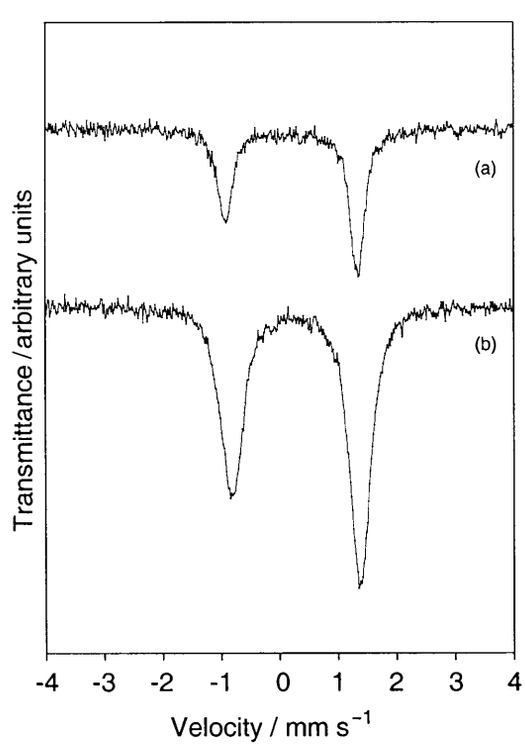

Fig. 6 ^{57}Fe Mössbauer spectra of $[Fe^{III}(TPP)]^{+}[TCNE]^{\bullet -}\cdot 2PhCl$ measured at (a) 290 K and (b) 77 K.

magneton (μ_B), θ = Weiss constant, k_B = Boltzmann constant, ρ = ratio of paramagnetic impurity, Na = temperature independent paramagnetism, $K = J/k_BT$, and $H = -2\Sigma J_{ij}\boldsymbol{S}_i\boldsymbol{S}_j$

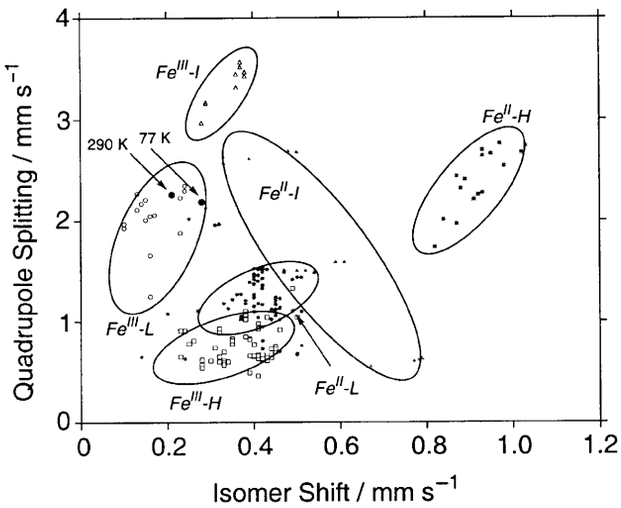

Fig. 7 Plot of Mössbauer parameters, quadrupole splitting and isomer shift, on a Maeda map;[55] ●, $[Fe^{III}(TPP)]^{+}[TCNE]^{\bullet -}\cdot 2PhCl$ (290 and 77 K); □, high-spin Fe^{III} (*Fe^{III} -H*); △, intermediate-spin Fe^{III} (*Fe^{III} -I*); ○, low-spin Fe^{III} (*Fe^{III} -L*), ■, high-spin Fe^{II} (*Fe^{II} -H*), ▲, intermediate-spin Fe^{II} (*Fe^{II} -I*); and ●, low-spin Fe^{II} (*Fe^{II}-L*). Each spin state region is circled using reference data.[54]

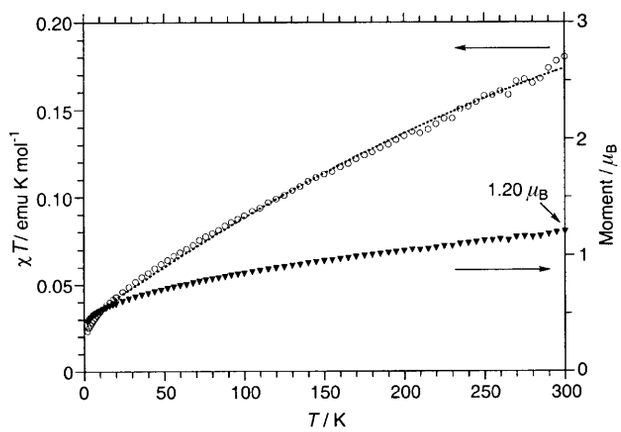

Fig. 8 χT (○) and magnetic moment (▼) as a function of temperature for polycrystalline $[Fe^{III}(TPP)][TCNE]$. The dotted line along χT is a fit using the Ising expression (1), with $J = -190$ cm^{-1}.

(spin Hamiltonian), for non-interacting chains comprised of alternating $g = 2$, $S = 1/2$ and $S = 1/2$ spins, with $J = -190$ cm^{-1} (Fig. 8).[58] Attempts to fit the data by a 1-D $S = 1/2$ Fisher model[58b] were unsuccessful. This strong antiferromagnetic interaction, attributable to the shorter $d(Fe–N^{TCNE})$ with respect to that of the manganese analogue, is more than five times larger than those for magnetically ordered $[Mn^{III}(por)]^{+}[TCNE]^{\bullet -}$ systems.[5]

Owing to the lack of an unpaired electron spin in the d_{z^2} orbital, spin coupling between the *z* component of the $[TCNE]^{\bullet -}$ pπ* orbital and the manganese(III) orbital, as attributed in $[Mn^{III}(por)]^{+}[TCNE]^{\bullet -}$, cannot occur.[11] Hence, a different spin coupling mechanism, most likely *via* the dπ (d_{zx}, d_{yz}) and $[TCNE]^{\bullet -}$ pπ* orbital, occurs.

Conclusion

$[Fe^{III}(TPP)]^{+}[TCNE]^{\bullet -}\cdot 2PhCl$ was prepared and structurally, spectroscopically, and magnetically characterized. Although the metal centered oxidation potential of Fe^{II}(TPP) was slightly positive shifted with respect to that of Mn^{II}(TPP), one electron is transferred from Fe^{II} to TCNE. The extremely short Fe–N^{TCNE} bond distance indicates that the iron is in the low-spin $(d_{xy})^2(d_{yz},d_{zx})^3$ state, which was confirmed by spectroscopic studies including ^{57}Fe Mössbauer. The unique properties associated with this Fe–N^{TCNE} coordination bonding were revealed as (i) a perpendicularly aligned ··· D–A–D–A ··· uniform 1-D supramolecular chain structure, (ii) the temperature dependent ν_{CN} stretching mode of $[TCNE]^{\bullet -}$, and (iii) strong antiferromagnetic interaction. In marked contrast to the σ-type $[Mn^{III}(por)]^{+}[TCNE]^{\bullet -}$ interactions, *i.e.*, molecular orbital interaction between d_{z^2} of the Mn^{III} and a nitrogen pπ* orbital of $[TCNE]^{\bullet -}$,[11,17] a π-type interaction between the dπ orbital of Fe^{III} and a pπ* orbital of $[TCNE]^{\bullet -}$ is the most plausible for $[Fe^{III}(TPP)]^{+}[TCNE]^{\bullet -}\cdot 2PhCl$.

Since the spin multiplicities of low-spin iron(III) ion and $[TCNE]^{\bullet -}$ are identical, strong antiferromagnetic interactions occur and magnetic ordering above 2 K was not observed. Hence, intermediate- and/or high-spin state iron(III) ion is required to generate a ferrimagnet. As the nitrogen containing $[TCNE]^{\bullet -}$ ligand has the possibility to induce both intermediate ($S = 3/2$)[59] and high-spin states ($S = 5/2$)[60] in a six-coordinated porphyrinatoiron(III) system, the ETS constructed from substituted Fe^{II}(TPP) and TCNE still has the potential to produce a new magnet. We are currently varying the incorporated solvent molecules and/or introducing substituents on the porphyrin ligand, as these strategies are well established methodologies to perturb structural properties of 1-D chains such as $d(M-N^{TCNE})$, angles $\angle M-NC^{TCNE}$, and those of P-TCNE. These structural perturbations may produce coordination geometries preferable to those of intermediate- and high-spin Fe^{III}, *e.g.* longer $d(Fe-N^{TCNE})$,[41] while maintaining the Fe–N^{TCNE} coordination bond.[14]

Experimental

General

TCNE (TCI Co., Ltd) was purified by vacuum sublimation. Chlorobenzene (Wako Pure Chemical, Inc.; >99%) and benzonitrile (PhCN) (Wako Pure Chemical, Inc.; >99%) were distilled under nitrogen over CaH_2. Dry pyridine (Aldrich) used for the synthesis and UV-vis studies was used without further purification. All manipulations were performed in a glove box with less than 1 ppm oxygen. Infrared spectra were recorded on a Perkin-Elmer System-2000 FTIR spectrometer in the range of 650 to 4000 cm^{-1} on NaCl discs as a mineral oil mull, temperature dependent IR spectra using a Daikin UV202A cryogenic refrigerating system in the temperature range from 15 to 300 K and absorption spectra with a Shimadzu UV-PC3100 spectrometer. Thermogravimetric analysis was performed with a Shimadzu TGA-50 instrument. The elemental analysis was made using a Perkin-Elmer 2400 apparatus. Cyclic voltammetry was performed with a BAS CV-50 set-up using glassy carbon working, platinum counter, and Ag–AgCl reference electrodes in $PhCN/^{n}Bu_4N^{+}PF_6^{-}$: $[Fe^{IV}(TPP)^{2-}]^{2+}$–$[Fe^{III}(TPP)^{2-}]^{+}$ +1.19, $[Fe^{III}(TPP)^{2-}]^{+}$–$[Fe^{II}(TPP)^{2-}]$ +0.14, and $[Fe^{II}(TPP)^{2-}]$–$[Fe^{I}(TPP)^{2-}]^{-}$ −1.12 V; TCNE–$[TCNE]^{\bullet -}$ +0.27 and $[TCNE]^{\bullet -}$–$[TCNE]^{2-}$ −0.79 V. The detailed conditions of the XPS,[61] Mössbauer,[62] and magnetic measurements[21] have been reported elsewhere.

Preparation of $[Fe^{III}(TPP)]^{+}[TCNE]^{\bullet -}\cdot 2PhCl$

A filtered hot solution of $[Fe^{II}(TPP)]$[38] (1.00 g, 1.50 mmol) in 200 mL of boiling chlorobenzene was added to TCNE (1.00 g, 7.81 mmol) in 200 mL of hot chlorobenzene. The solution was left to stand for two days, and the black-purple plate crystals that formed were collected by vacuum filtration and dried under vacuum for 3 h (yield: 900.0 mg, 59%). Calc. for $[Fe^{III}(TPP)]^{+}[TCNE]^{\bullet -}\cdot 2PhCl$, $C_{62}H_{38}Cl_2FeN_8$: C, 72.88; H, 3.75; Cl, 6.94; N, 10.97%. Found: C, 72.60; H, 3.63; Cl, 6.69; N, 11.03%.

Crystallography

The crystal data for $[Fe^{III}(TPP)]^{+}[TCNE]^{\bullet -}\cdot 2PhCl$ are

Table 3 Crystallographic data for $[Fe^{III}(TPP)]^{+}[TCNE]^{\bullet -}\cdot 2PhCl$

Formula	$C_{62}H_{38}Cl_2FeN_8$
M_r	1021.79
Crystal system	Triclinic
Space group	$P\bar{1}$ (no. 2)
μ(MoKα)/cm^{-1}	4.68
a/Å	10.937(4)
b/Å	13.320(4)
c/Å (≡ 1-D chain direction)	9.628(3)
α/°	97.17(3)
β/°	114.87(2)
γ/°	99.74(3)
V/Å^3	1223.8(8)
T/K	226.0(4)
Z	1
Measured/independent reflections	5923/5625
R	0.079
R(int)	0.014

summarized in Table 3. The temperature was calibrated with an Anritsu HFT-50 thermometer. Data were collected on a Rigaku AFC7R four circle diffractometer with graphite monochromated Mo-Kα radiation (λ = 0.71070 Å), and a Rigaku low temperature device. The ω–2θ scan technique was used.

CCDC reference number 186/2291.

See http://www.rsc.org/suppdata/dt/b0/b007931f/ for crystallographic files in .cif format.

Acknowledgements

This work was supported in part by a Grant-in-Aid for Scientific Research on Priority Area (no. 12023226 "Metal-assembled Complexes" to K.-i. S., no. 12042250 "Molecular Physical Chemistry" to K.-i. S., no. 10146103 "Creation of Characteristic Delocalized Electronic Systems" to Y. S., COE Research to Y. S., as well as no. 12440178 to K.-i. S. and no. 12440199 to Y. S.) from the Ministry of Education, Science, Sports and Culture, Japan, a Basic Research 21 for Breakthroughs in Info-communications (to K.-i. S.) from the Ministry of Posts and Telecommunications, and U.S. NSF Grant no. CHE-9320478 to J. S. M. It was also supported by grants from the Izumi Science & Technology Foundation (to K.-i. S.) and the Sumitomo Foundation (to K.-i. S.). We thank W. Hoffman for fitting the magnetic data to several models as well as helpful discussions with Dr Satoshi Takara, ISIR, Osaka University. We appreciate the technical assistance provided by the Materials Analysis Center of ISIR, Osaka University.

References

1 Recent reviews: (*a*) J. S. Miller and A. J. Epstein, *Chem. Commun.*, 1998, 1319; (*b*) J. S. Miller and A. J. Epstein, *Adv. Chem. Ser.*, 1995, **245**, 161; (*c*) J. S. Miller and A. J. Epstein, *Chem. Eng. News*, 1995, **73** 30; (*d*) J. S. Miller and A. J. Epstein, *Angew. Chem., Int. Ed. Engl.*, 1994, **33**, 385; (*e*) D. Gatteschi, *Adv. Mater.*, 1994, **6**, 635; (*f*) M. Kinoshita, *Jpn. J. Appl. Phys. Part 1*, 1994, **33**, 5718; (*g*) O. Kahn, in *Molecular Magnetism*, VCH Publishers, Weinheim., 1993; (*h*) R. Chiarelli, A. Rassat, Y. Dromzee, Y. Jeannin, M. A. Novak and J. L. Tholence, *Phys. Scr. T*, 1993, **49**, 706; (*i*) A. Caneschi and D. Gatteschi, *Prog. Inorg. Chem.*, 1991, **37**, 331; (*j*) V. I. Ovcharenko, R. Z. Sagdev, *Russ. Chem. Rev.*, 1999, **68**, 345; (*k*) J. S. Miller, *Inorg. Chem.*, 2000, **39**, 4392.

2 J. S. Miller, J. C. Calabrese, A. J. Epstein, R. W. Bigelow, J. H. Zhang and W. M. Reiff, *J. Chem. Soc., Chem. Commun.*, 1986, 1026.

3 R. D. Jones, D. A. Summerville and F. Basolo, *J. Am. Chem. Soc.*, 1978, **100**, 4416.

4 J. S. Miller, J. C. Calabrese, R. S. McLean and A. J. Epstein, *Adv. Mater.*, 1992, **4**, 498.

5 D. K. Rittenberg and J. S. Miller, *Inorg. Chem.*, 1999, **38**, 4838.

6 D. K. Rittenberg, K.-i. Sugiura, Y. Sakata, S. Mikami, A. J. Epstein and J. S. Miller, *Adv. Mater.*, 2000, **12**, 126.

7 J. S. Miller, C. Vazquez, J. C. Calabrese, R. S. Mclean and A. J. Epstein, *Adv. Mater.*, 1994, **6**, 217.

8 J. S. Miller, C. Vazquez, N. L. Jones, R. S. McLean and A. J. Epstein, *J. Mater. Chem.*, 1995, **5**, 707.

9 A. Böhm, C. Vazquez, R. S. McLean, J. C. Calabrese, S. E. Kalm, J. L. Manson, A. J. Epstein and J. S. Miller, *Inorg. Chem.*, 1996, **35**, 3083.

10 K.-i. Sugiura, S. Mikami, T. Tanaka, M. Sawada, J. L. Manson, J. S. Miller and Y. Sakata, *Chem. Lett.*, 1997, 1071.

11 E. J. Brandon, C. Kollmar and J. S. Miller, *J. Am. Chem. Soc.*, 1998, **120**, 1822.

12 E. J. Brandon, A. M. Arif, B. M. Burkhart and J. S. Miller, *Inorg. Chem.*, 1998, **37**, 2792.

13 E. J. Brandon, D. K. Rittenberg, A. M. Arif and J. S. Miller, *Inorg. Chem.*, 1998, **37**, 3376.

14 E. J. Brandon, A. M. Arif, J. S. Miller, K.-i. Sugiura and B. M. Burkhart, *Cryst. Eng.*, 1998, **1**, 97.

15 D. K. Rittenberg, K.-i. Sugiura, Y. Sakata, I. A. Guzei, A. L. Rheingold and J. S. Miller, *Chem. Eur. J.*, 1999, **5**, 1874.

16 K.-i. Sugiura, K. Ushiroda, M. T. Johnson, J. S. M. Miller and Y. Sakata, *J. Mater. Chem.*, 2000, **10**, 2507.

17 C. M. Wynn, M. A. Gîrtu, K.-i. Sugiura, E. J. Brandon, J. L. Manson, J. S. Miller and A. J. Epstein, *Synth. Met.*, 1997, **85**, 1695.

18 M. A. Gîrtu, C. M. Wynn, K.-i. Sugiura, E. J. Brandon, J. L. Manson, J. S. Miller and A. J. Epstein, *Synth. Met.*, 1997, **85**, 1703.

19 M. A. Gîrtu, C. M. Wynn, K.-i. Sugiura, J. S. Miller and A. J. Epstein, *J. Appl. Phys.*, 1997, **81**, 4410.

20 E. J. Brandon, K.-i. Sugiura, A. M. Arif, L. Liable-Sands, A. L. Rheingold and J. S. Miller, *Mol. Cryst. Liq. Cryst.*, 1997, **305**, 269.

21 K.-i. Sugiura, A. M. Arif, D. K. Rittenberg, J. Schweizer, L. Öhrstrom, A. J. Epstein and J. S. Miller, *Chem. Eur. J.*, 1997, **3**, 138.

22 C. M. Wynn, M. A. Gîrtu, J. S. Miller and A. J. Epstein, *Phys. Rev. B*, 1997, **56**, 315.

23 C. M. Wynn, M. A. Gîrtu, J. S. Miller and A. J. Epstein, *Phys. Rev. B*, 1997, **56**, 14050.

24 C. M. Wynn, M. A. Gîrtu, W. B. Brinckerhoff, K.-i. Sugiura, J. S. Miller and A. J. Epstein, *Chem. Mater.*, 1997, **9**, 2156.

25 A. J. Epstein, C. M. Wynn, M. A. Gîrtu, W. B. Brinckerhoff, K.-i. Sugiura and J. S. Miller, *Mol. Cryst. Liq. Cryst.*, 1997, **305**, 321.

26 E. J. Brandon, R. D. Rogers, B. M. Burkhart and J. S. Miller, *Chem. Eur. J.*, 1998, **4**, 1938.

27 K.-i. Sugiura, S. Mikami, M. T. Johnson, J. S. Miller, K. Iwasaki, K. Umishita, S. Hino and Y. Sakata, *Chem. Lett.*, 1999, 925.

28 K.-i. Sugiura, S. Mikami, M. T. Johnson, J. S. Miller, K. Iwasaki, K. Umishita, S. Hino and Y. Sakata, *J. Mater. Chem.*, 2000, **10**, 959.

29 D. K. Rittenberg, K.-i. Sugiura, A. M. Ariff, Y. Sakata, C. D. Incarvito, A. L. Rheingold and J. S. Miller, *Chem. Eur. J.*, 2000, **6**, 1811.

30 M. T. Johnson, A. M. Arif and J. S. Miller, *Eur. J. Inorg. Chem.*, 2000, 1781.

31 Cr^{III}: the bulk ferrimagnetic ordering of the corresponding high-spin chromium(III) (S = 3/2) complex, $[Cr^{III}(TPP)][TCNE]$, was reported: S. Sellers, B. Conklin and G. Yee, *Abstracts of Papers, Fourth International Conference on Molecular-Based Magnets*, Salt Lake City, 1994, Abstract p. 98; Mg^{II}: K.-i. Sugiura, Y. Sakata and J. S. Miller, unpublished work; other metals: J. S. Miller, unpublished work.

32 J. S. Miller, J. C. Calabrese, H. Rommelmann, S. R. Chittipeddi, J. H. Zhang, W. M. Reiff and A. J. Epstein, *J. Am. Chem. Soc.*, 1987, **109**, 769.

33 G. A. Candela, L. J. Swartzendruber, J. S. Miller and M. J. Rice, *J. Am. Chem. Soc.*, 1979, **101**, 2755.

34 G. T. Yee, J. M. Manriquez, D. A. Dixon, R. S. McLean, D. M. Groski, R. B. Flippen, K. S. Narayan, A. J. Epstein and J. S. Miller, *Adv. Mater.*, 1991, **3**, 309.

35 W. E. Broderick, J. A. Thompson, E. P. Day and B. M. Hoffman, *Science*, 1990, **249**, 410.

36 A. Wolberg and J. Manassen, *J. Am. Chem. Soc.*, 1970, **92**, 2982; J.-H. Fuhrhop, K. M. Kadish and D. G. Davis, *J. Am. Chem. Soc.*, 1973, **95**, 5140; K. M. Kadish, M. M. Morrison, L. A. Constant, L. Dickens and D. G. Davis, *J. Am. Chem. Soc.*, 1976, **98**, 8387.

37 The boundary of the ionic–neutral ground state of the ETS is $\Delta E = +0.17$ V using electrochemical redox potentials, *i.e.* ionic ground state $\Delta E < +0.17$ V, neutral ground state $\Delta E > +0.17$ V: T. J. B. Torrance, J. E. Vazquez, J. J. Mayerle and V. Y. Lee, *Phys. Rev. Lett.*, 1981, **46**, 253.

38 H. Kobayashi and Y. Yanagawa, *Bull. Chem. Soc. Jpn.*, 1972, **45**, 450.

39 $[Fe^{II}(TPP)]$ exhibits a reversible one-electron oxidation at +0.14 V (*vs.* Ag–AgCl, in PhCN), and hence can reduce TCNE (E^{RED} = +0.28 V *vs.* Ag–AgCl), to form $[Fe^{III}(TPP)]^{+}[TCNE]^{\bullet -}$.[37]

40 M. P. Byrn, C. J. Curtis, Y. Hsiou, S. I. Khan, P. A. Sawin, S. K. Tendick, A. Terzis and C. E. Strouse, *J. Am. Chem. Soc.*, 1993, **115**, 9480.
41 W. R. Scheidt and Y. J. Lee, *Struct. Bonding (Berlin)*, 1987, **64**, 1.
42 F. A. Walker, H. Nasri, I. Turowska-Tyrk, K. Mohanrao, C. T. Watson, N. V. Shokhirev, P. G. Debrunner and W. R. Scheidt, *J. Am. Chem. Soc.*, 1996, **118**, 12109.
43 J. Silver, P. J. Marsh, M. C. R. Symons, D. A. Svistunenko, C. S. Frampton and G. R. Fern, *Inorg. Chem.*, 2000, **39**, 2874.
44 O. Q. Munro, J. A. Serth-Guzzo, I. Turowska-tyrk, K. Mohanrao, T. K. Shokhireva, F. A. Waker, P. G. Debrunner and W. R. Scheidt, *J. Am. Chem. Soc.*, 1999, **121**, 11144.
45 O. Q. Munro, H. M. Marques, P. G. Debrunner, K. Mohanrao and W. R. Scheidt, *J. Am. Chem. Soc.*, 1995, **117**, 935.
46 D. A. Dixon and J. S. Miller, *J. Am. Chem. Soc.*, 1987, **109**, 3656.
47 G. T. Yee, J. C. Calabrese, C. Vazquez and J. S. Miller, *Inorg. Chem.*, 1993, **32**, 377.
48 V. Gutmann, in *The Donor–Acceptor Approach to Molecular Interactions*, Plenum, New York, 1978, ch. 1.
49 Out-of-register refers to parallel chains with D's (donor molecules) near A's (acceptor molecules) and A's near D's, and in-register refers the chain with D's near D's and A's near D's.
50 K. Nakamoto, in *Infrared and Raman Spectra of Inorganic and Coordination Compounds 5th Edition (Part B)*; John Wiley & Sons, New York, 1997, p. 113.
51 A. Johnson and H. Taube, *J. Indian Chem. Soc.*, 1989, **66**, 503.
52 M. K. Safo, G. P. Gupta, C. T. Watson, U. Simonis, F. A. Walker and W. R. Scheidt, *J. Am. Chem. Soc.*, 1992, **114**, 7066.
53 The absorption attributable to $[TCNE]^{\bullet -}$ typically observed at 24,000 cm^{-1} was not determined; ref. 46.
54 J. R. Sams and T. B. Tsin, in *The Porphyrins Vol. IV*, ed. D. Dolphin, Academic Press, New York, 1979, p. 425.
55 Y. Maeda, *J. Phys. Colloq.*, 1979, **C2–40**, 514.
56 XPS: C 1s 284.6, N 1s 398.53, Fe $2p_{1/2}$ 721.8, and Fe $2p_{3/2}$ 708.3 eV. The observed binding energy (BE) for Fe $2p_{3/2}$ of the ETS, 708.3 eV, is closer to values reported for iron(III), 708.5–709.7 eV, than for iron(II) porphyrins, 706.6–706.9 eV: A. J. Signorelli and R. G. Hayes, *J. Chem. Phys.*, 1976, **64**, 4517. However, it was pointed out that both the BEs for Fe $2p_{1/2}$ and Fe $2p_{3/2}$ of porphyrinatoiron complexes are not sensitive to their oxidation states: K. Ichimura, Y. Nakahara, K. Kimura and H. Inokuchi, *J. Mater. Chem.*, 1992, **2**, 1185.
57 The EPR *g* values for powdered $[Fe^{III}(TPP)]^{+}[TCNE]^{\bullet -}\cdot 2PhCl$ are 2.0 and 3.1 at 77 K.
58 (*a*) O. Kahn, in *Molecular Magnetism*, VCH Publishers Inc., Weinheim, 1993, ch. 11; E. Sinn, *Coord. Chem. Rev.*, 1970, **5**, 313. The exchange interaction, *J*, was as -190 cm^{-1}, $g = 2.0$, $\theta = -4$ K, $\rho = 0.18$ (%) by minimizing $R = [\Sigma\ (\mu_{obs} - \mu_{calc})^2/\Sigma\ \mu_{obs}^2]^{\frac{1}{2}}$; (*b*) J. C. Bonner and M. E. Fisher, *Phys. Rev.*, 1964, **135**, A640.
59 D. A. Summerville, I. A. Cohen, K. Hatano and W. R. Scheidt, *Inorg. Chem.*, 1978, **17**, 2906.
60 D. K. Geiger, Y. J. Lee and W. R. Scheidt, *J. Am. Chem. Soc.*, 1984, **106**, 6339.
61 S. Hino, K. Umishita, K. Iwasaki, K. Tanaka, T. Sato, T. Yamabe, K. Yoshizawa and K. Okahara, *J. Phys. Chem. A*, 1997, **101**, 4346.
62 M. Manago, S. Hayami, Y. Yano, K. Inoue, R. Nakata, A. Ishida and Y. Maeda, *Bull. Chem. Soc. Jpn.*, 1999, **72**, 2229.